Multielectron Spectroscopy: The Xenon 4*d* Hole Double Auger Decay

F. Penent, J. Palaudoux, P. Lablanquie, and L. Andric
LCP–MR, Université Pierre et Marie Curie, 11, rue P et M Curie, 75231 Paris, France

R. Feifel and J. H. D. Eland
PTCL, Oxford University, Oxford, United Kingdom
(Received 28 April 2005; published 17 August 2005)

A magnetic bottle spectrometer of the type recently developed by Eland *et al.* [Phys. Rev. Lett. **90**, 053003 (2003).] has been implemented for use with synchrotron radiation, allowing multidimensional electron spectroscopy. Its application to the Xe 4*d* double Auger decay reveals all the energy pathways involved. The dominant path is a cascade process with a rapid (6 fs) ejection of a first Auger electron followed by the slower (> 23 fs) emission of a second Auger electron. Weaker processes implying 3 electron processes are also revealed, namely, direct double Auger and associated Rydberg series.

DOI: 10.1103/PhysRevLett.95.083002 PACS numbers: 32.80.Hd, 32.70.Fw

Core photoionization is an efficient way to investigate matter, as both the photoelectron ejected from the core hole and the subsequently emitted electrons convey information on the target. It is the interpretation of the photoelectric effect by Einstein in 1905 [1] that opened the way to the study of the structure of energy levels. Photoelectron spectroscopy, that is, removal of an electron by a photon, was then used to explore not only valence shells but also inner shells [2]. However, core holes result in short-lived highly excited species, and Auger [3] discovered that their deexcitation can occur either by radiative decay or by emission of secondary electrons, the so-called Auger electrons. Auger spectroscopy is widely used today both in basic research and in material science [4]. Coincidence detection of the photoelectron and a subsequent Auger electron have proved useful in studies of both solid and diluted species to sort out overlapping inner-shell hole decay paths, and to go beyond the two step description implied in the above description [5–8]. Yet these studies have remained limited, and a multielectron spectroscopy that unites photoelectron and Auger electron spectroscopies and present complete multidimensional energy maps of all emitted electrons has still to be developed.

Such a multielectron Auger spectroscopy method is presented here and is used to elucidate the case where a shallow inner shell hole decays by emission of more than one Auger electron. Deep inner shells are known to decay by cascade emission of Auger electrons, corresponding to transitions between successive inner-shell levels [9], while the first accessible inner shell is expected to decay by emission of a single Auger electron only. A weaker channel was, however, discovered in noble gazes, with emission of 2 electrons: the double Auger process [10]. Its interest lies in the strong electron correlation from which it originates. One important question concerns its dynamics: is it a direct double Auger process where both Auger electrons emitted simultaneously share continuously the excess energy, or is it a cascade process with subsequent emission of electrons of well defined energies? Recently coincidence experiments addressed this point [11,12], but they were restricted to limited coincidences between two released electrons, whereas coincidence detection of all three electrons is necessary for a complete characterization.

We present here a new experiment in which all released electrons (here up to three) are detected in coincidence and resolved in energy. Applied to the xenon photoionization, it enables us to get a complete picture of the energetics of the 4*d* hole decay, and especially to reveal the complete two-dimensional spectra of the double Auger decay path, hitherto unknown.

The multielectron spectrometer is a smaller version (2.4 m instead of 5 m) of the one developed in Oxford [13]. Its principle is the measurement of electrons' times of flight in a magnetic bottle [14] with a position sensitive detector coupled to a multihit time-to-digital converter. The interaction zone is located close to the pole of a strong (0.5 T) permanent magnet (NdFeB) adjustable in position, whose field guides essentially all emitted electrons through a long solenoid (5 G) towards the detector. Photoionization is brought by synchrotron light produced by the SA31 grazing incidence beam line from the Super ACO storage ring in Orsay, France. The two-bunch operation mode of the synchrotron was used, providing a 120 ns period between light pulses. This high repetition rate prevents the direct measurement of electron times of flight that can extend up to a few microseconds. However, these can be reconstructed in specific circumstances, such as Auger processes created with photons of known high excess energies: the trick is that the fast photoelectrons have known kinetic energies, so that their absolute times of flight can be reconstructed even if measured modulo the small interpulse period. Absolute times of flight of subsequent Auger electrons, detected in coincidence with the photoelectron, are then automatically obtained, and Auger electron energies can be unambiguously deduced. Calibration of the time to energy conversion was obtained with Xe Auger

lines of known energies [15] and by measuring the arrival time of zero energy electrons. Compared to other similar methods that collect all electrons, such as the ones that combine homogeneous electric and magnetic fields [16,17], angular information is here sacrificed in favor of high energy resolution, which is energy dependent and varies from 20 meV at low electron energies (< 1 eV) to 100 meV at 10 eV.

Figure 1 displays the complete two-dimensional energy map of the double Auger decay of the Xe $4d$ holes, created by photoionization. To ensure that the photoelectrons are faster than any Auger electrons, 110.4 eV photons were chosen . We consider here only those events where all three electrons associated with double Auger processes are detected. The time of flight of the first, rapid photoelectron enables one to recognize which sublevel ($4d_{3/2}$ or $4d_{5/2}$) was created. Strong electron correlation is already evident from the intensity of this double Auger decay path compared to the one where only one Auger electron is emitted. The constant transmission of our spectrometer as a function of electron energies enables us to extract this information directly from the number of coincidence events, taking into account the electron detection efficiency. We obtain for this ratio of double to single Auger probabilities, values of $34 \pm 5\%$ and $20 \pm 4\%$, respectively, for the $4d_{3/2}$ and $4d_{5/2}$ decays, in good agreement with estimates from photoelectron-ion coincidence experiments [18,19]. The two-dimensional surfaces of Fig. 1 show strongly structured lines of constant Auger energy sum, associated with different Xe^{3+} final states. These are revealed by projecting Fig. 1 along the $x = y$ diagonal, as in Fig. 2. Lorentzian broadening of the peaks, due to the finite lifetime of the $4d$ holes (6.3 ± 0.2 fs for $4d_{3/2}$ and 5.9 ± 0.2 fs for $4d_{5/2}$) [20] is clearly seen. Relative positions of the Xe^{3+} states are found to be in good agreement with spectroscopic tables [21]. The probability for populating each state is reported in Table I. Statistical branching ratios for this double autoionization process are not observed, contrary to the double photoionization case [13], although configuration mixing [21] may redistribute intensities among all $j = 3/2$ Xe^{3+} states. Low excess energies may also be the origin of the low $2P_{3/2}$ population and of the lower relative intensity of the $Xe^{3+2}D_{5/2}$ states when populated by $4d_{5/2}$ decay rather than by $4d_{3/2}$, and, in fact, observed branching ratios are surprisingly close to the ones expected in a crude Wannier model [22].

As the binding energies of the $Xe^{+}4d^{-1}$ states have been accurately measured (within ± 12 meV) [23], our experiment determines the absolute binding energies of the Xe^{3+} states, and leads to a value of 64.09 ± 0.04 eV for the triple ionization threshold in xenon. Note that previous direct measurements of this threshold show large scatter and error bars: electron impact estimates vary from 64.35 ± 0.10 eV [24] to 66.15 ± 0.10 eV [25] while a photoionization experiment reported 64.1 ± 0.3 eV [26]. Our method is more accurate and also more reliable than indirect determination

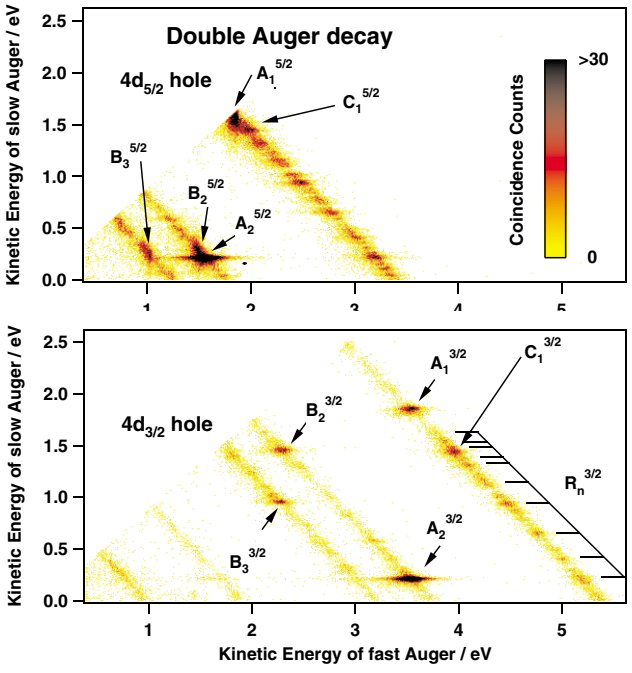

FIG. 1 (color online). Decay of xenon $4d$ holes by emission of two Auger electrons. All three electrons of the process are detected in coincidence. The two-dimensional plot of the Auger double continua are filtered according to the associated photoelectron. Intensity color scale was selected to enhance structures. Maximum count is 186 ($4d_{3/2}$ case) or 248 ($4d_{5/2}$). Scattered points as well as the horizontal lines at about 0.2 eV are due to false coincidences.

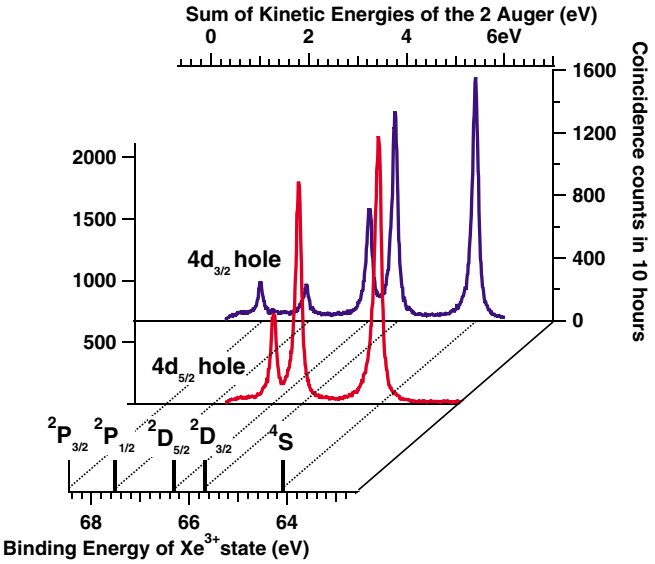

FIG. 2 (color online). Histogram of the sum of the two Auger energies following a $4d$ hole, as deduced from integration along the diagonal lines of Fig. 1. The histogram can be referenced to the $Xe^{+}4d^{-1}$ energy levels [23] to yield the binding energies of the final Xe^{3+} states (bottom axis).

TABLE I. Branching ratios (BR) for the formation of Xe^{3+} states by double Auger decay of the Xe $4d$ holes.

	$^4S_{3/2}$	$^2D_{3/2}$	$^2D_{5/2}$	$^2P_{1/2}$	$^2P_{3/2}$
$4d_{3/2}$	100	80	50	10	10
$4d_{5/2}$	100	70	30		
Stat.[a]	100	100	150	50	100
Wan.$4d_{3/2}$[b]	100	68	58	34	17
Wan.$4d_{5/2}$[b]	100	50	35		

[a]Statistical BR $(2j + 1)$.
[b]BR from available phase space in Wannier model [22].

obtained from the analysis of emission lines that give the position of the Xe^{2+} ground state at 33.105 eV [5] and its ionization potential at 31.05 ± 0.04 eV [21], i.e., 64.105 ± 0.04 eV.

Figure 3 gives one-dimensional double Auger spectra filtered according to both the initial hole and the Xe^{3+} final states, deduced by plotting intensities along the coincidence lines of Fig. 1, as a function of E_1 and E_2. Intensity is dominated by peaks lying on a weak continuum, attributed to direct double Auger process. The peaks reveal that sequential ejection of the Auger electrons dominates this ''double autoionization process'' in a similar way to autoionization in double photoionization of the noble gases [13,27]. These cascade decays can be rationalized by considering the intermediate Xe^{2+} states X. Each may give rise to various spots on Fig. 1 labeled X_i^s, depending on whether the state is populated from the $4d$ level $s = 3/2$ or $5/2$ and decays to the Xe^{3+} level $i = 1$ to 5 (taken in order of increasing binding energy). Such X_i^s spots correspond to a pair of Auger electrons, $(1X_i^s, 2X_i^s)$, where $1X_i^s$ denotes the energy of the first emitted Auger electron. This will present a Lorentzian profile when projected as in Fig. 3, due to the $4d_s$ hole lifetime. The $2X_i^s$ electron, on the other hand, will reflect the lifetime of the intermediate X state. In spite of some experimental, energy dependent broadening due to the time of flight technique, we observe that intermediate states are of longer lifetime than the $4d$ holes, giving thinner second Auger lines. Furthermore, if $1X_i^s > 2X_i^s$, then we expect a horizontal spot in Fig. 1, which is the case for most of the peaks, but a vertical spot when $1X_i^s < 2X_i^s$, as observed for peaks $A_1^{5/2}$, $B_2^{5/2}$, and $B_3^{5/2}$. With the help of properties such as $1X_i^{3/2} = 1X_i^{5/2} + SO_{4d}$ with $SO_{4d} = 4d$ spin-orbit splitting, or $2X_i^s = 2X_j^s + SO_{ij}$ with SO_{ij} splitting of the Xe^{3+} levels i and j, it is possible to reconstruct the cascade trees from Fig. 1. It appears that 2 dominant Xe^{2+} states A and B, of binding energies 66.00 and 67.27 eV, are the origins of most structures and represent 33% of all double Auger decays. A is the most intense and can decay to the Xe^{3+} ground (^4S) and first excited ($^2D_{3/2}$) states, with the release of a second Auger electron of $2A_1^{5/2} = 2A_1^{3/2} = 1.85$ eV or $2A_2^{5/2} = 2A_2^{3/2} = 0.22$ eV, respectively, and branching ratios of (73/27), directly obtained from relative peak areas. Peak shape of this second electron is affected by the resolution of our apparatus and by the lifetime of the Xe^{2+} intermediate state, which is found to be longer than 23 fs; see Fig. 3. Apart from these 2 states, a series of Xe^{2+} states is visible in Fig. 1 decaying to the Xe^{3+} ground state. Their intensities as observed in the $4d_{3/2}$ double Auger map and in Fig. 3 suggest a Rydberg series of R_n Xe^{2+} states converging onto the $(2D_{3/2})$ Xe^{3+} state, except for the structure labeled C_1^s. We propose that the strong Xe^{2+} intermediate states A, B, and C are the last members of the correlation Auger satellites of $5s^{-2}$ configuration [28], and result from an Auger decay of the $4d$ holes by a 2 electron process

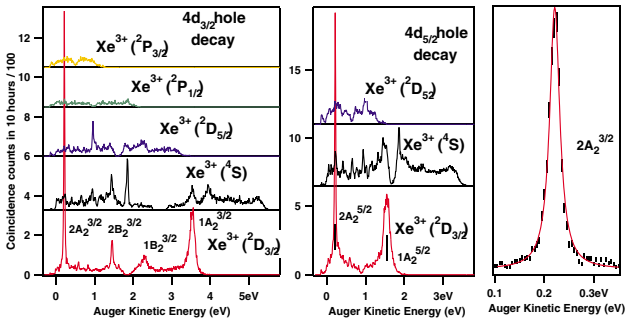

FIG. 3 (color online). One-dimensional double Auger spectra associated with the formation of the specified Xe^{3+} final states, through double Auger decay of the $4d_{3/2}$ (left) or $4d_{5/2}$ (middle) hole, and deduced from Fig. 1. Right: an enlargement of the $2A_2^{3/2}$ peak from the left panel, fitted with a Lorentzian function of 28 meV FWHM. As experimental broadening is not included, it implies a Xe^{2+} intermediate A of a lifetime longer than $\tau = 1/28$ meV = 23 fs. Zero intensities in the middle of each spectrum, at equal Auger energies result from the 150 ns dead time of the detector.

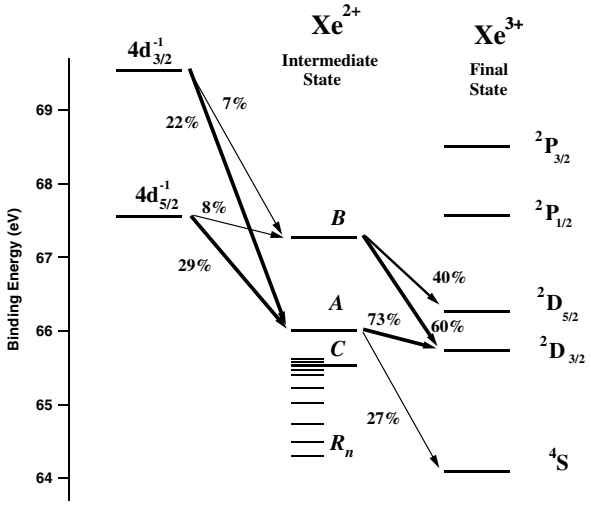

FIG. 4. Scheme for the main decay of the $4d$ holes by cascade emission of two Auger electrons.

involving two 5*s* electrons. By contrast, the R_n Rydberg series implies higher electron correlation and a true 3 electron process, similar to the double Auger process they are the precursors of. Figure 4 summarizes the decay paths revealed in this study. Theoretical investigations are clearly needed to reproduce the double Auger continuum and investigate the nature of the resonant decay paths.

Finally, complete Auger spectra of the 4*d* decays can be obtained by considering all 2 electron coincidence events where a 4*d* photoelectron and an Auger electron have been detected, as reported in [29]. They are similar to the traditional Auger spectra ([28] and references therein), but filtering of the hole helps sort out Auger lines and makes possible the observation of the complete Auger spectra down to zero kinetic energy. The double Auger part of the spectra can be simply deduced by scaling the results obtained from triple electron coincidence events.

As a conclusion, implementation with synchrotron radiation of the magnetic bottle multielectron spectrometer introduced in Oxford [13] has been demonstrated to reveal energetics and dynamics of Xe 4*d* double Auger decay. This apparatus is expected to be of general interest for multiple Auger processes in atoms and molecules. Furthermore, significant dynamical energy exchange with Auger pair (postcollision interaction process) are expected when the photoelectron escapes with low energy. A study of such effects is under way using the unique properties of this apparatus and is expected to provide a detailed view of 3 electron interactions.

LURE staff are warmly acknowledged for providing the last Super ACO photons in autumn 2003. We are indebted to O. Jagutzi for his efficient help on the Roentdek position sensitive detector, and to Professor L. Cederbaum and Professor K. Ito for stimulating discussions.

[1] A. Einstein, Ann. Phys. (Leipzig) **17**, 132 (1905).
[2] K. Siegbahn *et al.*, Nova Acta Regiae Soc. Sci. Ups. **20**, 1 (1967).
[3] P. Auger, J. Phys. Radium **6**, 205 (1925).
[4] W. Mehlhorn, J. Electron Spectrosc. Relat. Phenom. **93**, 1 (1998).
[5] V. Schmidt, *Electron Spectrometry of Atoms Using Synchrotron Radiation* (Cambridge University Press, Cambridge, 1997).
[6] J. Viefhaus *et al.*, Phys. Rev. Lett. **80**, 1618 (1998).
[7] P. Lablanquie *et al.*, Phys. Rev. Lett. **84**, 47 (2000).
[8] A. Liscio *et al.*, J. Electron Spectrosc. Relat. Phenom. **137**, 505 (2004), and references therein.
[9] A. G. Kochur, A. I. Dudenko, and I. D. Petrov, J. Phys. B **37**, 2401 (2004), and references therein.
[10] T. A. Carlson and M. O. Krause, Phys. Rev. Lett. **14**, 390 (1965).
[11] P. Lablanquie *et al.*, Phys. Rev. Lett. **87**, 053001 (2001).
[12] J. Viefhaus *et al.*, Phys. Rev. Lett. **92**, 083001 (2004).
[13] J. H. D. Eland *et al.*, Phys. Rev. Lett. **90**, 053003 (2003).
[14] P. Kruit and F. H. Read, J. Phys. E **16**, 313 (1983).
[15] T. X. Carroll *et al.*, J. Electron Spectrosc. Relat. Phenom. **125**, 127 (2002).
[16] R. Dorner *et al.*, Phys. Rep. **330**, 95 (2000).
[17] M. Gisselbrecht *et al.*, Rev. Sci. Instrum. **76**, 013105 (2005).
[18] B. Kammerling, B. Krassig, and V. Schmidt, J. Phys. B **25**, 3621 (1992).
[19] N. Saito and I. H. Suzuki, J. Phys. Soc. Jpn. **66**, 1979 (1997).
[20] M. Jurvansuu, A. Kivimaki, and S. Aksela, Phys. Rev. A **64**, 012502 (2001).
[21] A. Tauheed, Y. N. Joshi, and E. H. Pinnington, Phys. Scr. **47**, 555 (1993).
[22] G. H. Wannier, Phys. Rev. **90**, 817 (1953).
[23] G. C. King *et al.*, J. Phys. B **10**, 2479 (1977).
[24] R. Dutil and P. Marmet, Int. J. Mass Spectrom. Ion Phys. **35**, 371 (1980).
[25] D. Mathur and C. Badrinathan, Phys. Rev. A **35**, 1033 (1987).
[26] J. H. D. Eland *et al.*, Z. Phys. D **4**, 31 (1986).
[27] P. Bolognesi *et al.*, J. Electron Spectrosc. Relat. Phenom. **141**, 105 (2004).
[28] J. Jauhiainen *et al.*, J. Phys. B **28**, 3831 (1995).
[29] F. Penent *et al.*, J. Electron Spectrosc. Relat. Phenom. **144–147**, 7 (2005).